Comparative study of the mass-loading effect on electrical parameters of gallium phosphate, quartz and langasite resonators

I. Mateescu[1]
[1]National Institute of Materials Physics
Bucharest, Romania

F. Krispel[2]
[2]Piezocryst Advanced Sensorics
Graz, Austria

S. Georgescu[3]
[3]National Institute for Laser, Plasma, and Radiation Physics,
Bucharest, Romania

K. Scott[4]
[4]Sawyer Technical Materials LLC
Eastlake, Ohio, USA

E. Borca[5]
[5]University of Bucharest, Romania

Abstract **– This paper presents some of the more relevant results concerning the mass-loading influence on the characteristics (effective mass-loading, motional inductance, quality factor) of AT-cut quartz, Y-cut langasite resonators and AT-cut gallium phosphate**

I. INTRODUCTION

The evolution of the electronic systems and especially the telecommunication systems towards higher frequencies and baud rates led to the necessity to find new solutions for the frequency generation and filtering devices.

The most frequently used piezoelectric crystals in these devices (quartz, lithium tantalate, lithium niobate) fulfill only partially these requirements. Quartz is stable with temperature and has low acoustic loss, but the low piezoelectric coupling factor makes it difficult to build compact broad band band-pass filters. On the contrary, lithium niobate has a high piezoelectric coupling factor, but the temperature drift is very large, undesirable for band-pass filters used in mobile communication systems [1, 2].

Recent reports of the prestigious scientists from Russia, USA, Japan, France have focused on langasite ($La_3Ga_5SiO_{14}$ - LGS) and its isomorphs langanite ($La_3Ga_{5.5}Nb_{0.5}O_{14}$ - LGN) and langatate ($La_3Ga_{5.5}Ta_{0.5}O_{14}$ - LGT), the new piezoelectric crystals from the calcium gallogermanate family. These crystals belong to the same crystallographic class as quartz (32) but accomplish better the desired properties.

Due to the excellent behavior with temperature, high piezoelectric coupling factor, low acoustic losses and absence of phase transitions up to their melting points (~1470°C), these crystals could be successfully used at high temperatures in resonant structures with bulk and surface acoustic waves [3, 4].

Since langasite and langatate crystals can be grown directly from the melt by the conventional Czochralski pulling method, large size crystals are commercially available. At present time only langasite is used for device production, while LGN and LGT are available only in small quantities for property evaluation [2, 5, 6].

Another new material, gallium phosphate ($GaPO_4$), is a promising piezoelectric material for high tech applications such as high temperature pressure sensors, viscosimeters, microbalances for chemical sensors, etc. [7, 8]. $GaPO_4$ [3] has a structure similar to α-quartz and presents improved physical properties compared with the quartz crystal. $GaPO_4$ belongs to the point group 32 and its structure is homeotypic to quartz, the silicon atoms from SiO_2 being replaced alternately with phosphorus and gallium. Since there is no α-β phase transition, $GaPO_4$ can be used up to 970ºC. At this temperature occurs a phase transition to a cristobalite-like structure. The $GaPO_4$ crystal extends at high temperatures the good properties of the quartz for sensor applications (no pyroelectric effect, high insulation resistance). The high density of this material (3570 kg/m^3) leads to a lower acoustic velocity and, thus, to a lower thickness of a resonator working at the same frequency. The high piezoelectric coefficient (double, compared to quartz) leads to a higher electromechanical coupling coefficient of $GaPO_4$ resonators with better results in SAW and BAW devices.

The study of the mass-loading effect on the electrical characteristics of resonators is based on the Ballato's transmission-line analog of the trapped-energy resonators vibrating in thickness-shear mode that can evidence the electrical parameters behavior on fundamental frequency and harmonics [9, 10].

As suggested in [13], the non-uniform distribution of motion is associated with the coupling of the thickness-shear and the thickness-twist modes, as well with the stress at the interface electrodes-piezoelectric substrate.

1-4244-0647-1/07/$20.00 ©2007 IEEE

This paper presents a comparative analysis of the more relevant results concerning the mass-loading influence on the characteristics of AT-cut quartz, Y-cut langasite and AT-cut gallium phosphate resonators.

II. MASS-LOADING EFFECT

The typical piezoelectric plate resonator [10] consisting of a disk with metallic electrodes top and bottom is shown in Fig. 1.

The piezoelectric plate of thickness $2h$ and density ρ_s contains some region A_a, known as the active area where the acoustic waves are driven by voltages applied to electrodes of thickness t_e (each side) and density ρ_e. The region where the electrodes overlap to form a parallel plate capacitor structure is denoted as the electroded area A_e.

The inertial interaction of electrodes and substrate is described by the ratio of electrode mass per unit area to substrate mass per unit area, denoted as mass-loading μ.

For the case of an infinite plate with no lateral variations, the electrode and active areas are coincident and the mass loading is given by the familiar form

$$\mu = \frac{\rho_e t_e}{\rho_s h} \qquad (1)$$

where mass-loading and electrode thickness are directly proportional.

In 1972 Ballato [9] proposed an exact transmission–line analog for a single thickness-shear mode in a piezoelectric resonator with a geometry of an infinite plan-parallel plate and with uniform distribution of motion. In the case of a single mode and small mass-loading, the resonance frequencies may be determined from

$$\frac{\tan X}{X} = \frac{1}{k^2 + \mu X^2} \quad , \quad X = \frac{\pi}{2} \frac{f_{R\mu}^{(M)}}{f_{A0}^{(1)}} \qquad (2)$$

and the antiresonance frequencies may be determined from

$$\frac{\tan X}{X} = \frac{1}{\mu X^2}, \quad X = \frac{\pi}{2} \frac{f_{A\mu}^{(M)}}{f_{A0}^{(1)}} \qquad (3)$$

Equations for large mass-loading are simply developed using the transmission line analog.

The mass-loading can be determined directly from "(3)", while the piezoelectric coupling can be obtained from "(2)".

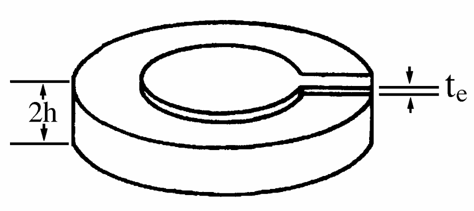

Fig.1. Piezoelectric plate resonator

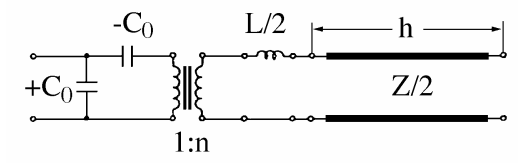

Fig.2. Transmission-line analog for single TETM mode

If the mass-loading is by definition a fixed ratio of densities, one should be able in theory to use the antiresonance frequencies of a series of harmonics to determine both mass-loading and the unloaded fundamental antiresonance frequency. In practice, however, the situation is complicated by the non-uniform distribution of vibratory motion, so that what we measure as antiresonance is actually the point where the integral of the current density taken over the electrode area vanishes . In order to explain the harmonic variations, it is necessary to examine the transmission-line analog being used [10].

The transmission-line analog for a single thickness-shear mode, in the case of thick electrode films, is shown in Fig. 2. Implicit in the calculation of the equivalent circuit elements are the assumptions of lateral unboundedness and a uniform distribution of motion. A simple first approximation to the real world case of lateral boundedness can be made by retaining the assumption of a uniform distribution of motion but allowing for a difference between the electroded area A_e, and the active area A_a.

The equivalent circuit elements are then calculated as

$$C_0 = \frac{\varepsilon_{22}^{S} A_e}{2h} \qquad (4)$$

$$n^2 = \frac{C_0 A_e c_m k^2}{2h} \qquad (5)$$

$$L = m A_e \qquad (6)$$

$$Z = A_e \sqrt{\rho c_m} \qquad (7)$$

In "(4)" through "(7)", a uniform plane wave of modal stiffness c_m and piezoelectric coupling k is considered to propagate in a piezoelectric plate of mass density ρ. The resonator geometry (Fig. 1) is characterized by the plate thickness *2h*, electrode area A_e and electrode mass per unit area *m*. It is also necessary to introduce the ratio between the electrode area and active area, denoted *b*.

If one uses "(4)" through "(7)" in finding the critical frequencies of the transmission-line analog of Fig. 2, one obtains "(8)" and "(9)" with the difference that the piezoelectric coupling k and mass loading μ are now replaced by effective values k_{eff} and μ_{eff}.

The effective coupling is given by :

$$k_{eff}^2 = \frac{k^2}{b} \qquad (8)$$

and the effective mass loading is given by:

$$\mu_{eff} = \mu b \frac{\tan X_e}{X_e} \qquad (9)$$

The effective mass-loading is the product of the "ideal case" mass-loading for thin films given by "(l)", the electroded fraction of the active area b, and a transcendental term relating to wave propagation in the case of thick films. The term X_e, is defined similarly to the X of "(2)" and "(3)", being equal to $\pi/2$ times the ratio of the critical frequency being measured to the fundamental antiresonance frequency of the total electrode film of thickness $2t_e$.

In [10], based on the Ballato's transmission-line analog, an accurate determination of the electrode mass-loading was performed. The discrepancies between the "effective" mass-loading deduced from the measured frequency spectrum and the mass-loading calculated from the physical and geometrical characteristics of the electrode and substrate, could be indicative for a non-uniform distribution of vibratory motion (NUDM) over the electrode area of the resonator.

Based on the experimental results obtained in [11, 12] the non-uniform distribution of motion could be ascribed to the effects associated to the electrode deposition at the interface electrode-piezoelectric substrate including defects and stresses.

In order to account for the non-uniform distribution of motion, found in usual plates resonators, in [13] was introduced a correction of the mass-loading and of the coupling coefficient using the Tiersten's analysis [14] of trapped-energy resonators vibrating in coupled thickness-shear and thickness-twist modes. The experimental results for AT-cut quartz resonators [11, 12] were in good agreement with the theory

From these results one can conclude that the non-uniform distribution of motion depending on electrode geometry could be ascribed to the coupling of the thickness-shear and thickness-twist modes and to the effects associated to the electrode deposition.

III. EXPERIMENTAL

Plan-parallel polished AT-cut quartz (Sawyer, USA), Y-cut langasite (Sawyer, USA), and AT-cut gallium phosphate (Piezocryst Advanced Sensorics, Austria) plates of 14 mm diameter and 5 MHz fundamental resonant frequency have been used in experiments.

Gold electrodes with 75, 150, 200 nm thickness and with 7 mm electrode diameters have been deposited on the blanks by thermal evaporation in vacuum using a JEOL - JEE 4X installation.

The resonance and anti-resonance frequencies and series resistances of the fundamental, 3rd, 5th and 7th overtones of the plates with and without electrodes were measured after each electrode layer deposition.

Using the relations for Ballato's transmission-line equivalent electrical circuit of the piezoelectric plate resonator vibrating in the thickness-shear mode, the effective mass-loading, piezoelectric coupling coefficient, motional inductance, motional capacitance and quality factor were calculated.

Mass-loading effect was evidenced by the change of these parameters with harmonics. Only the most relevant parameters i.e., effective mass-loading, motional inductance and quality factor, have been studied in this paper. The electrode deposition of the resonators investigated in this paper was performed in same experimental conditions.

IV. RESULTS

A comparison between the experimentally results of the mass-loading influence on AT-cut quartz, Y-cut langasite, and AT-cut gallium phosphate resonators characteristics was performed.

The harmonic dependence of the effective mass-loading, motional inductance and quality factor for various electrode parameters has been analyzed.

A. *Effective mass-loading μ_{eff}*

In Fig. 3 is presented the effective mass-loading variation with harmonic order for all types of resonators (AT-cut quartz, Y-cut langasite, and AT-cut gallium phosphate) with Au electrodes of 7 mm diameter and 150 nm thickness.

The effective mass-loading behavior of AT-cut quartz resonators is different from those of Y-cut langasite, and AT-cut gallium phosphate resonators. Thus, while the effective mass-loading of quartz resonators increases with harmonics, that of langasite, and gallium phosphate decreases.

B. *Motional inductance L*

The variation with harmonics of the motional inductance for all types of resonators with the same electrode parameters (material, thickness) is presented in Fig. 4.

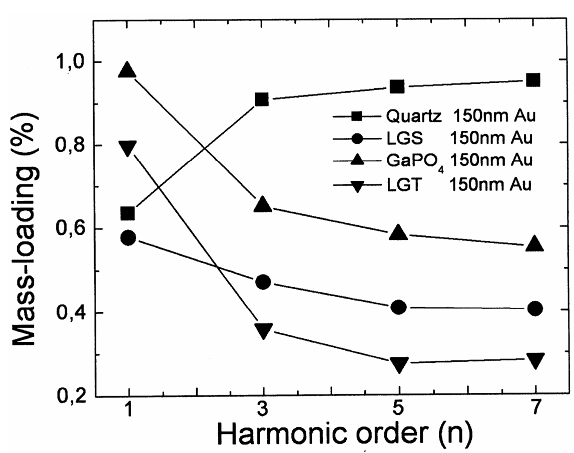

Fig.3. Effective mass-loading variation with n

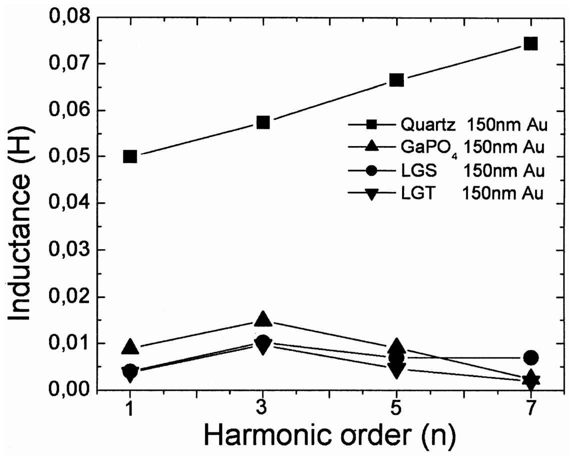

Fig. 4. The harmonic dependence of the inductance L

This figure shows that the inductance of AT-cut quartz resonators has a significant change with harmonics, while the inductance of Y-cut langasite, and AT-cut gallium phosphate presents only a small change at third harmonics.

C. *Quality factor Q*

The quality factor values of AT-cut quartz, Y-cut langasite, Y-cut langatate, and AT-cut gallium phosphate deposited with Au electrodes of 7 mm diameter and 150 nm thickness are given in Fig.5.

An analysis of the Fig. 5 reveals that for this electrode thickness (150 nm) the quality factor reaches its maximum value for the third harmonics.

The highest value of the quality factor is obtained for Y-cut langasite resonators followed by AT-cut quartz resonators and, with practically the same values, by AT-cut gallium phosphate.

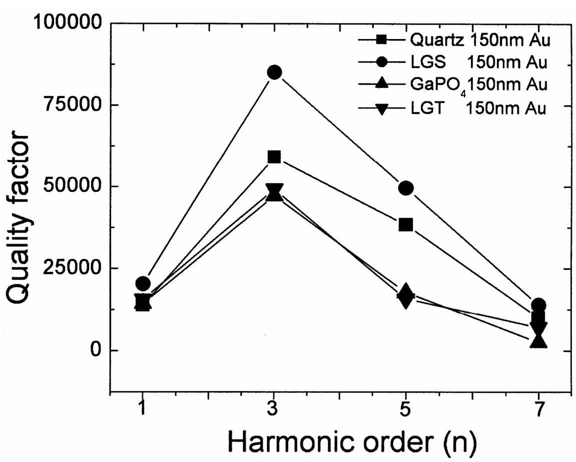

Fig. 5. The quality factor variation on harmonics

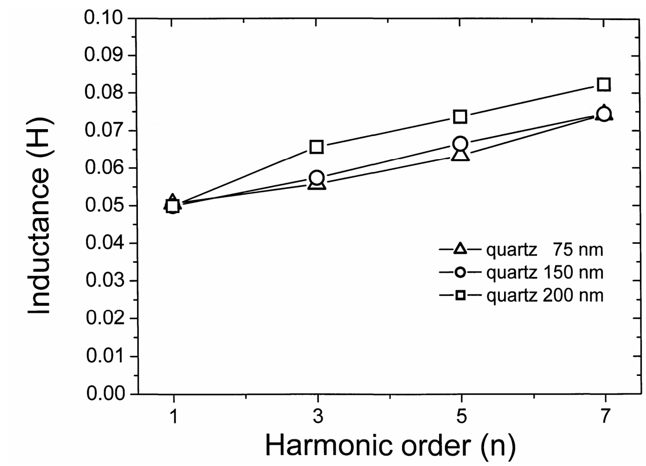

Fig. 6. Harmonic variation of quartz resonators inductance

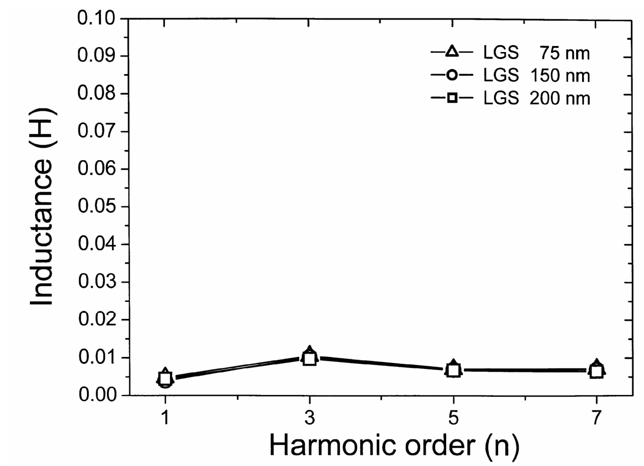

Fig. 7 Inductance dependence on harmonic order for Y-cut LGS resonators

In Fig. 6 is presented the harmonic dependence of inductance for AT-quartz resonators of various electrode thickness (75, 150, 200 nm).

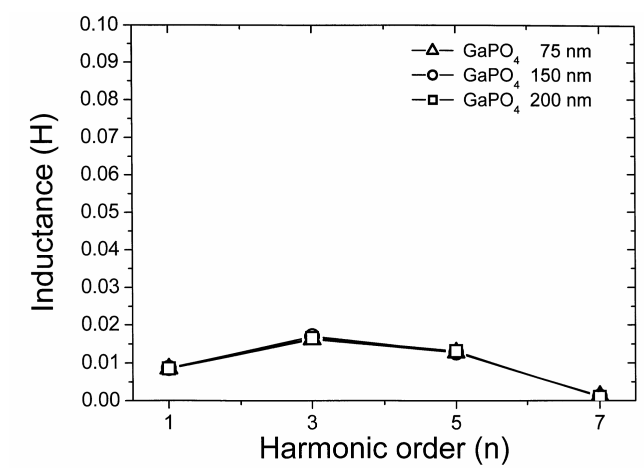

Fig.8. Inductance variation with harmonics for AT-cut $GaPO_4$ resonators

The behavior of the inductance L with harmonic order for Y-cut langasite resonators with the same electrode thicknesses is shown in Fig.7.

In Fig.8 the variation with harmonic order of $GaPO_4$ resonators with 75, 150, 200nm electrode thickness is presented.

Analysing the harmonic dependence of inductance L for AT-cut quartz, Y-cut langasite and AT-cut $GaPO_4$ resonators with various electrode thickness, one observe that the change of inductance of AT-cut quartz resonators with electrode thickness is higher than that of Y-cut LGS and AT-cut of $GaPO_4$ resonators.

These observations, compared to the previous experimental and theoretical results [11, 12, 13], allow to assign the increase of the inductance with order of overtone to the decrease of the active area of AT-cut quartz resonators due to the non-uniform distribution of motion under electrodes. On the other side the non-uniform distribution of motion is partially determined by stresses at interface electrode-piezoelectric substrate. The relation between inductance and internal stress allows to suppose that the inductance behavior for different types of resonators with various electrode thickness can be ascribed to peculiar stresses.

These results suggest that the Y-cut langasite and AT-cut gallium phosphate resonators develop a smaller interface stresses than AT-cut quartz resonators.

V. CONCLUSIONS

The experimental results obtained in this study allow concluding that the mass-loading influence on Y-cut langasite and AT-cut gallium phosphate resonators is much smaller than in the case of the AT-cut quartz resonators.

The analysis of these resonators revealed the following differences between AT-cut quartz resonators, on the one side, and Y-cut langasite, and AT-cut gallium phosphate resonators, on the other side:

- effective mass-loading increases with harmonics for AT-cut quartz resonators and decreases for the other ones;

- maximum variation of the inductance is significantly lower for Y-cut langasite, and AT-cut gallium phosphate resonators than for AT-cut quartz resonators;

- for all these resonators the maximum value of the quality factor was obtained for the third harmonics.

Based on our previous results [11,12] according to which the inductance change with mass-loading is due to the internal stress at interface electrode-piezoelectric substrate, we could ascribe the specific behavior of inductance of Y-cut langasite, and AT-cut gallium phosphate to a much smaller interfacial stresses in comparison with AT-cut quartz resonators.

ACKNOWLEDGEMENTS

This work was supported by the Romanian Education and Research Ministry (Contract CEEX 28/2006).

REFERENCES

[1] H. Takeda, K. Sugyama, K. Inaba, K. Shimamura and T. Fukuda, "Crystal growth and structural characterization of new piezoelectric material $La_3Ta_{0.5}Ga_{5.5}O_{14}$", Jpn. J. Appl. Phys. Vol. 36 ,1997, pp. 919-92.

[2] B. Chai, J. L. Lefaucheur, Y. Y. Ji and H. Qiu, "Growth and evaluation of large size LGS ($La_3Ga_5SiO_{14}$), LGN ($La_3Ga_{5.5}Nb_{0.5}O_{14}$) and LGT ($La_3Ga_{5.5}Ta_{0.5}O_{14}$) single crystals", Proc. IEEE. Int. Freq. Contr. Symp., 1998, pp. 748-752.

[3] J. Detaint, J. Schwartzel, A. Zarka, B. Capelle, J. P. Denis, E. Philippot, "Bulk wave propagation and energy trapping in the new thermally compensated materials with trigonal symmetry", Proc. IEEE Int. Freq. Contr. Symp., 1994, pp. 58-71.

[4] R. C. Smythe, R. C. Helmbold, G. E. Hague, K. A. Snow, "Langasite, langanite and langatate bulk-wave Y-cut resonators", IEEE Trans. UFFC 47, nr.2, 2000, pp. 355-360.

[5] C. Klemenz, M. Berkowski, B. Deveaud - Pledran, D. C. Malocha, "Defect structure of langasite-type crystals: a challenge for applications", Proc. IEEE Int. Freq. Contr. Symp., 2002, pp. 301-306.

[6] Yu. V. Pisarevsky, P. A. Senyushenkov, B. V. Mill, N. A. Moiseeva, "Elastic, piezoelectric, dielectric properties of $La_3Ga_{5.5}Ta_{0.5}O_{14}$ single crystal", Proc. IEEE Int. Freq. Contr. Symp., 1998, pp. 742-746.

[7] F. Krispel, H. Thanner, P. W. Krempl, C. Reiter, P. M. Worsch, W. Wallnofer, "$GaPO_4$ resonators with Q factors of some millions in the fundamental mode", Proc. IEEE Int. Freq. Contr. Symp., USA, 2002, pp. 342-346.

[8] F. Krispel, C. Reiter, J. Neubig, P. W. Krempl, F. Lenzenhuber, W. Wallnofer, P. M. Worsch, "Properties and applications of single rotated $GaPO_4$ resonators", Proc. IEEE Int. Freq. Contr. Symp. and European Frequency and Time Forum, USA, 2003, pp. 668-673.

[9] A. Ballato, "Transmission-line analogs for stacked piezoelectric crystal devices", Proc. 26th Ann. Symp. Freq. Contr., USA, 1972, pp. 86-91.

[10] J. Kosinski, A. Ballato, S. Mallikarjun, "Mass-loading measurements of quartz crystal plates", Proc. 43rd Ann. Symp. Freq. Contr, USA, 1989, pp. 365-371.

[11] I. Mateescu, E. Candet, "Non-uniform distribution of motion influence on the effective mass-loading in AT-cut quartz resonators", Proc. IEEE Freq. Contr. Symp., 1992, pp.561-565.

[12] I. Mateescu, I.V..Mateescu, "Complex mass-loading effects in AT-cut quartz crystal resonators", Proc. European Frequency and Time Forum, 1993, pp.63-65.

[13] J.Kosinski, A. Ballato, I. Mateescu,"Inclusion of non-uniform distribution of motion effects in the transmission-line analogs of the piezoelectric plate resonators: theory and experiment" Proc. IEEE Int. Freq. Contr. Symp., USA, 1994, pp. 229-236.

[14] H. F. Tiersten, Journal of the Acoustical Society of America, **59,** 1976